JOURNAL OF AIRCRAFT
Vol. 30, No. 3, May–June 1993

Flapping Motion of a Planar Jet Impinging on a V-Shaped Plate

Cheng-Kuang Lin*
Chung Shan Institute of Science and Technology, Taichung, Taiwan, Republic of China
and
Fei-Bin Hsiao† and Shyh-Shiun Sheu‡
National Cheng Kung University, Tainan, Taiwan, Republic of China

The behavior of a planar jet impinging on a V-shaped plate is studied experimentally by means of pressure and velocity measurements and flow visualization. The plate with a symmetrically variable opening angle is located downstream at distance L from the jet exit. Data indicate that, for the presence of the plate, not only the large-scaled coherent structures in the shear layers exist in the jet, but also the whole jet column exhibits a prominent periodic flapping motion with a preferred frequency f_F in the flowfield. Results also show an unstable regime occurring for the flapping motion, in which the criteria to determine the boundary of the regime are governed by the location and the opening angle of the plate. Moreover, the nondimensional Strouhal number $f_F L/U_j$ is found to maintain a constant value of 0.11, and this value is nearly insensitive to the opening angle of the plate in the operating Reynolds number range.

Nomenclature

f_F = flapping frequency of the jet column motion
H = jet height at the exit
L = impinging length or the plate location
l = coordinate along the wide-angle plate
$p_i(t)$ = dynamic pressure fluctuations at $l = i \times 1.5H$
$p_{\text{rms},i}$ = root-mean-squared value of $p_i(t)$
Re = Reynolds number ($U_j H/\nu$)
St = Strouhal number ($f_F L/U_j$)
U_j = jet exit velocity
V_c = streamwise fluctuating velocity at the jet center
X = coordinate along streamwise direction
Y = coordinate along transverse direction
θ = opening angle of the V-shaped plate
ν = kinematic viscosity

Introduction

THE evolution of flow behaviors for a freejet has been extensively studied for several decades.[1–3] The dynamics and the merging mechanism of the jet have been well-documented in the literature. However, for a jet impinging on a solid boundary, the flow behaviors would become very complicated. The flow structures and their characteristics of the jet associated with the solid boundary still remain unclear to us. As one considers the practical applications of this kind, such impinging jets play an important role in the fuel and gas mixing for combustion, thrust vectoring for V/STOL aircraft, etc.

For a circular jet impinging on a flat plate, Ho and Nossier[4] experimentally found that pressure waves which are propagating upstream could form a feedback loop with coherent structures traveling downstream in the flowfield between the jet exit and the plate. Hence, the large-scaled and small-scaled vortices would be collectively interacting with each other to enhance the flow mixing. Didden and Ho[5] also observed that unsteady flow separation could occur within the boundary layer of the flat plate as the vortical structures impinged on the plate. As a result, secondary vortices were then induced by the primary vortices. These results were also observed in the impinging planar jet with a flat plate by Hsiao, et al.[6] The above papers were all related to the study of the jet impingement on a flat plate located in the near field. However, Gutmark et al.[7] investigated a planar jet with a flat plate located in the far field, $100H$. They found that the flow properties on the jet centerline were essentially the same as in a freejet in the near field. The vortex stretching phenomenon was significant near the impinging plate, but no jet flapping motion was reported. A concise review concerning the self-sustained oscillations of impinging free shear layers had been well-presented by Rockwell and Naudascher.[8] Rockwell[9] further surveyed various aspects of impinging and nonimpinging free shear flows from the experiments and the theoretical analyses. Staubli and Rockwell[10] recently studied the interaction of an unstable planar jet with an oscillating wedge. Very detailed physical insights and simple mathematical models were provided with the relation between impinging vortical structures and pressure fluctuations.

At the present time, most of the papers reviewed[4,5,9,10] are concentrated on the jet or shear layer impingement on a flat plate or a wedge. There is no literature that concerns the flow behaviors of the jet when impinging on a V-shaped plate as shown in Fig. 1. In this case, since a larger pressure field may be developed due to the plate having an opening angle facing the flow directly, the jet within the flowfield may perform different behaviors as compared to an impinging jet with a flat plate[4,5] or a wedge.[10] Thus, the purpose of this article is to investigate, through pressure and velocity measurements and flow visualization, the characteristics of the flapping motion of a planar jet when they are impinging on a downstream V-shaped, varying opening angle plate. The results of these investigations can be applied directly to a cooling system in which the jet is impinging on a V-shaped surface or a similar concaved surface. The understanding of the characteristics of the impinging jet flapping motion may also be useful for the thrust vectoring control or lift augmentation in aircraft design. The parameters of study will include the exit velocity of the jet (U_j), the distance of the plate from the jet exit (L), and the opening angle of the plate (θ).

Received Oct. 17, 1991; revision received March 4, 1992; accepted for publication March 4, 1992.

*Scientist, Aeronautical Research Laboratory.
†Professor, Institute of Aeronautics and Astronautics. Member AIAA.
‡Ph.D. Candidate, Institute of Aeronautics and Astronautics.

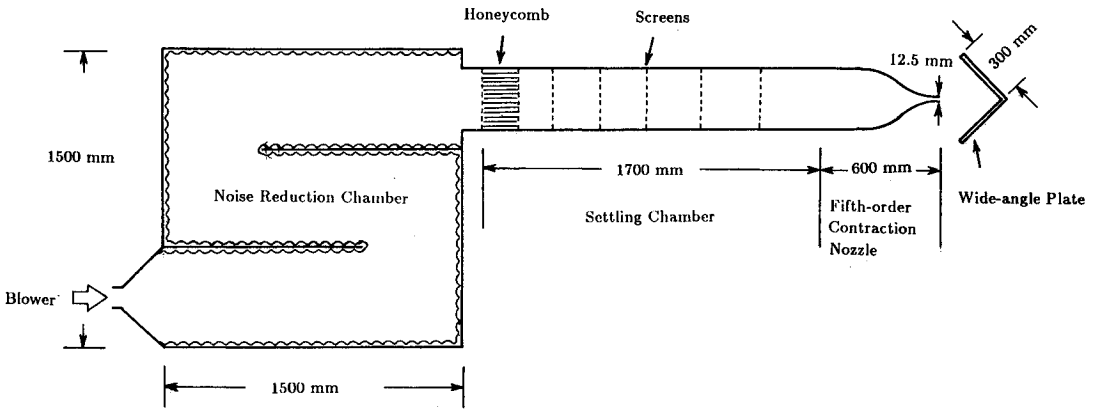

Fig. 1 Experimental setup of the impinging planar jet.

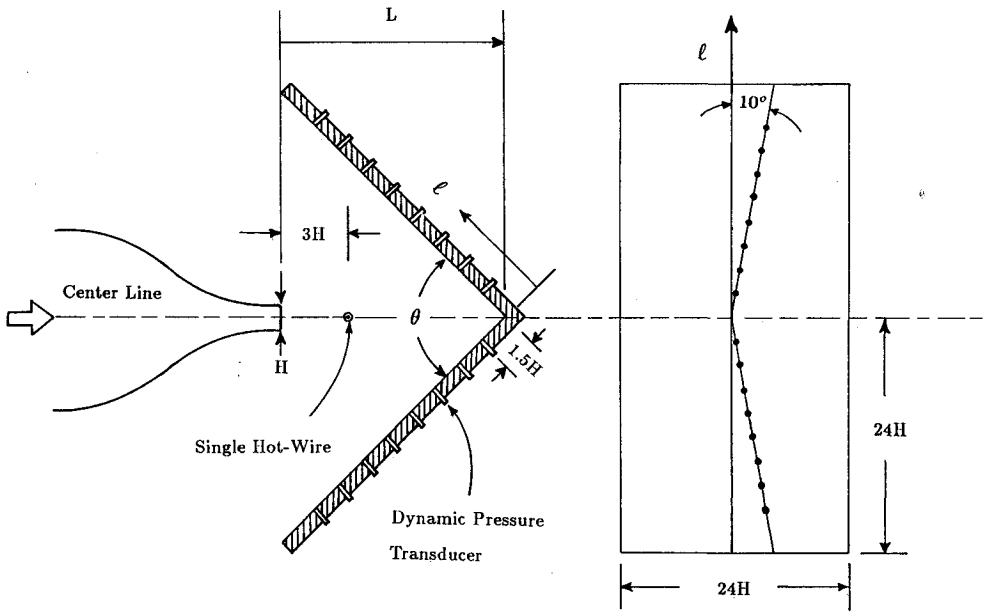

Fig. 2 Schematic diagram of the impinging jet and the sensor locations.

Experimental Facilities

The experimental setup of the planar jet is shown in Fig. 1. The jet facility includes a blower, a noise-reduction chamber, a settling chamber, and a contraction nozzle. The air is driven by a 3-hp centrifugal blower with a variable speed controller. The noise-reduction chamber is composed of a circulation-looped duct and buffles, all covered with acoustic-absorbing foam rubber to diminish the passage noise from the blower. The settling chamber contains a set of honeycomb and five screens for further flow uniformity and turbulence intensity managements. The nozzle profile is fitted with a fifth-order polynomial curve. The height of the jet (H) at the nozzle exit is 12.5 mm with an aspect ratio of 24 (see Fig. 2). The jet exit velocity is varied from 1 to 30 m/s. The corresponding Reynolds number based on the jet height is between 8.3×10^2 and 2.5×10^4. The impinging plate with symmetrically variable opening angle is constructed by two flat plates hinged together. Both plates have the same dimensions, 300 by 500 mm. The opening angle can be adjusted from 0 to 180 deg. The plate is moved along the centerline of the jet by a traversing mechanism. Dynamic pressures are directly measured from ENDEVCO-8507 dynamic pressure transducers which are flush-mounted on the plates as indicated in Fig. 2. A single hot-wire with DANTEC 55M01 anemometer is used to detect the velocity signals at the jet center. All the data are acquired and processed by a personal computer.

For the study of the flow structure development, a planar water jet facility is also used along with the application of the coloring-dye injection technique. The whole setup is quite similar to the design for the air jet as described, except for the water jet is vertically mounted, and the tunnel and the nozzle are completely immersed in a large reservoir to avoid the free surface effect on the flow development. The nozzle is of 4.0 mm in height at the jet exit, which has an aspect ratio of 24. The jet speed ranges from 5 to 100 cm/s with the corresponding Reynolds number between 2.0×10^2 and 4.0×10^3. The pictures of the flow structures are taken through a video camcorder and a 35-mm photography camera with a 150-W floodlight.

Results and Discussion

Flow Behavior of the Flapping Jet

For a water jet having an exit velocity of 0.13 m/s ($Re = 5.2 \times 10^2$) impinging on a flat plate, located $10H$ downstream, the jet column is observed to behave in an almost symmetrical pattern with respect to the centerline of the jet. When approaching the boundary of the plate, the jet column is then divided into two transversely opposite streams along the flat plate. This is shown in Fig. 3. A locally high pressure field is developed on the plate and secondary vortices are easily induced after the boundary layer is separated. This picture also

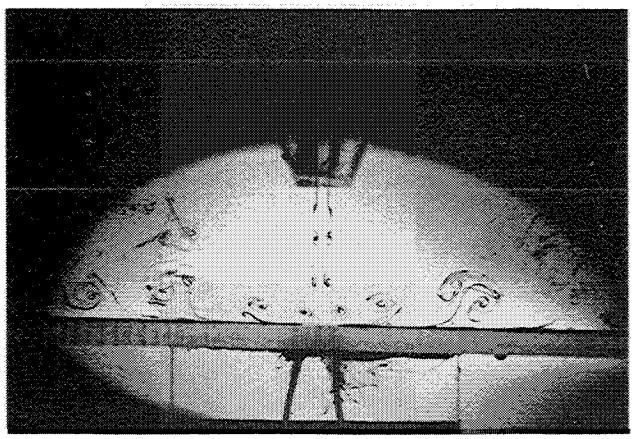

Fig. 3 Flow patterns of the impinging jet with a flat plate for L/H = 10 and U_j = 0.13 m/s.

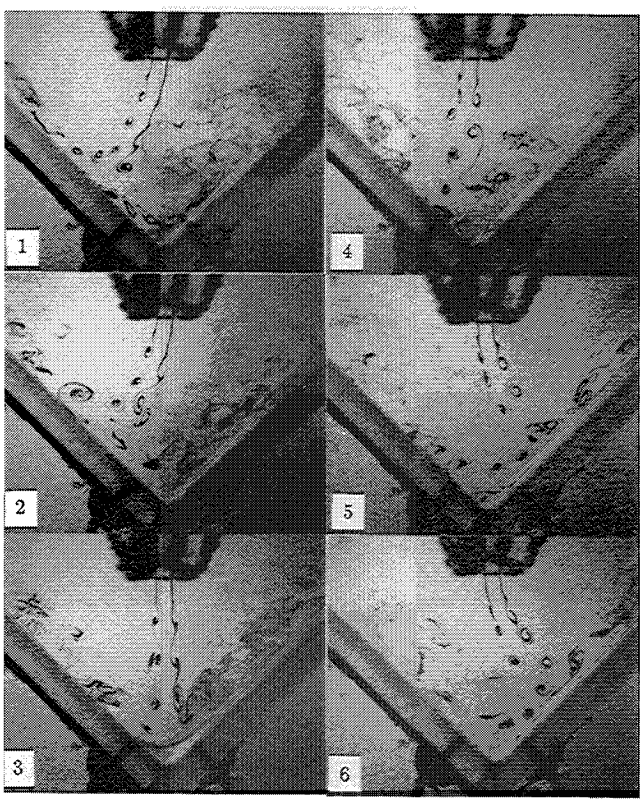

Fig. 4 Sequential flow developments of the impinging jet with 0.2 s difference for U_j = 0.21 m/s, L = 10H, and θ = 90 deg.

clearly illustrates the secondary vortices along with the primary vortices in the vicinity of the plate. More detailed phenomena were discussed by Didden and Ho[6] and recently by Hsiao et al.[7] When the jet impinges on a V-shaped 90-deg opening angle plate (again located 10H downstream), a distinct flapping motion of the impinging jet is observed as seen in Fig. 4 where sequential flow patterns of the impinging jet over time are depicted. The pictures here demonstrate a half-cycle of the flapping motion. It is noted that the large-scaled coherent structures in the shear layers evolved from the Kelvin-Helmholtz instabilities coexists with the flapping motion of the jet column.[3,6] They appear quite persistent and locally organized even as approaching the impinging plate. The flapping frequency is estimated to be about 0.5 Hz, which is very close to the value obtained by the pressure measurements. However, the corresponding fundamental frequency of the shear layer vortices is about 20 times higher than the flapping frequency of the jet column. The more detailed discussion

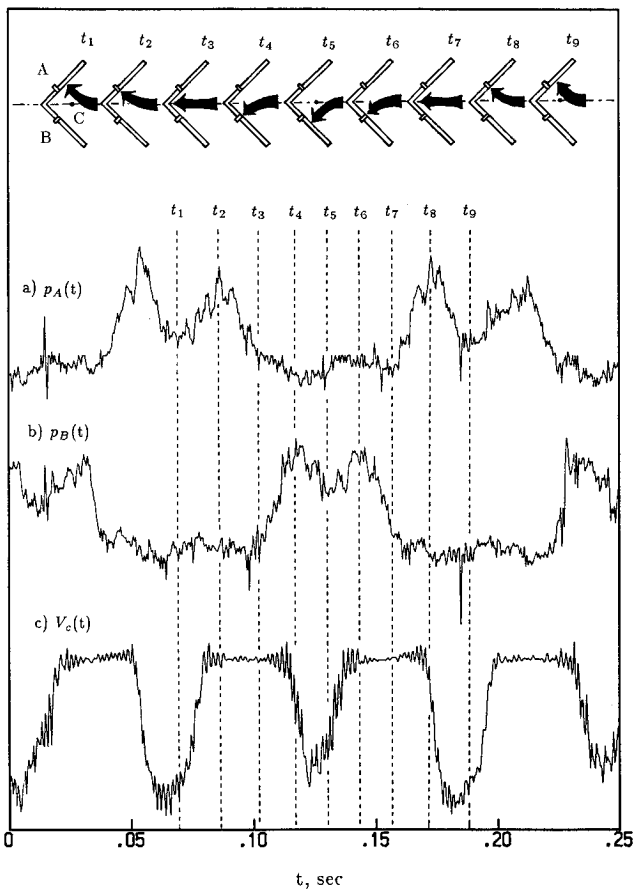

Fig. 5 Typical oscillograms of the jet flapping motion for a) pressure fluctuations at point A, b) pressure fluctuations at point B, and c) velocity fluctuations at point C, 3H downstream from the nozzle exit, when U_j = 10 m/s, L/H = 10 and θ = 90 deg.

will be in the next few sections through pressure and velocity measurements.

Characteristics of Pressure and Velocity Signatures During the Flapping Motion

In order to characterize the jet flapping behaviors as discussed in the previous section, detailed pressure and velocity measurements are performed by employing the dynamic pressure transducers and hot-wire anemometer. Figure 5 demonstrates the typical pressure and velocity oscillograms along with the schematic illustrations of the flapping jet at the time the plate is located 10H downstream and U_j = 10 m/s. Figures 5a and 5b depict the pressure fluctuations, which are respectively measured at points A and B on the plate (i.e., l = $\pm 3H$), and Fig. 5c for the velocity fluctuations at the jet center, point C, 3-H downstream from the jet exit. All of these results exhibit a relevant periodic characteristics for the jet flapping motion as was discussed in the flow visualization study previously. Figures 5a and 5b also show a time lag of half-period of the jet flapping in-between. Since the measuring points A and B are located symmetrically about the jet centerline, the half-period time lag implies that the jet column flaps in an antisymmetrical fashion with respect to the jet center. In this figure, nine particular instants of time, from t_1 to t_9, are marked, which are associated with the corresponding jet flapping motion in one cycle. The initial time t_1 is chosen when the jet column reaches the most outward flapping position, where p_A attains a local minimum. When the jet column flaps to point A at t_2, p_A increases to a local maximum due to the flapping jet passing by. Meanwhile, p_B starts to increase drastically when the jet column just crosses the centerline at t_3. It then reaches a local maximum as soon as the jet column comes to point B at t_4. Again, p_B decreases

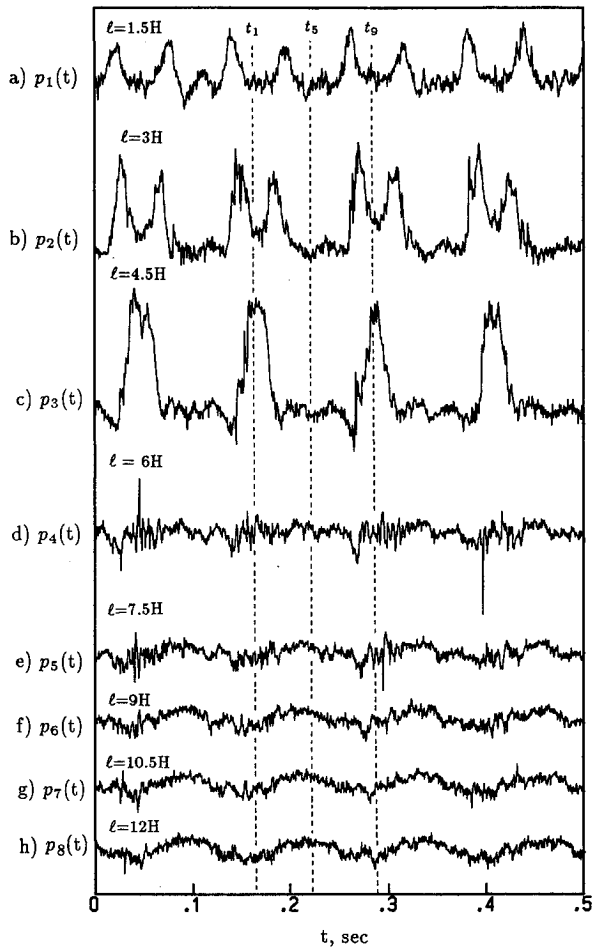

Fig. 6 Dynamic pressure fluctuations on the plate at various positions for U_j = 10 m/s, L/H = 10 and θ = 90 deg.

to a local minimum when the jet column attains the most outward position at t_5. Thereafter, the jet column alters its direction and flaps back to the original side in the same feature of the pressure variations. Once the jet column goes back to t_9, a complete cycle of the flapping motion is finished. Likewise, the jet column goes on flapping periodically and regularly in this fashion. It is also interesting to investigate the behavior of the velocity fluctuation V_C in Fig. 5c, which is measured at the jet center, point C. When the jet column reaches the most outward positions t_1, t_5, and t_9, V_C would correspond to local minima, respectively. As for when the jet column passes the centerline, point C, either at t_3 or t_7, V_C exhibits a maximal plateau with a duration of time. Since the measuring point C is exposed to the potential core region of the jet column in this case, V_C attains the jet exit velocity during the time interval when the flapping jet comes across the jet center region. It is also noticeable that there are high frequency fluctuations modulated with the low frequency fluctuations, both in the velocity and the pressure signals. In the energy spectral analysis (see Fig. 11), these high frequency fluctuations are contributed by the passages of the large-scaled coherent structures evolved from the Kelvin-Helmholtz instabilities upstream. This is also evident as depicted in Fig. 4.

Meanwhile, to study the behaviors of the dynamic pressure fluctuations in detail along the plate, eight pressure transducers are flush-mounted on the plate with equal spacing, $1.5H$, measured from the hinged point of the wide-angle plate. Figure 6 presents the pressure fluctuations from p_1 to p_8 for the impinging plate at $10H$ and U_j = 10 m/s. These results can be specifically classified into three different kinds of behaviors which depend upon the characteristics of the oscillograms. From p_1 to p_3, the oscillation amplitudes are large and the pressure fluctuations contain two peaks in one period, as compared with the rest of the pressure fluctuations. The high amplitude behavior is clearly due to the impingement of the jet column. As explained previously, the existence of these two pressure peaks between t_1–t_9 is mainly due to two impingements on the pressure sensors in one cycle of the flapping motion. For p_3, these two peaks are about to merge into one peak. This corresponds to the location where the flapping jet is approaching the extreme amplitude of the jet motion. Thus, the amplitude of the flapping jet motion is determined to be about $4.5H$ in this case. The second category is for p_4, in which the low frequency variation is not so clear. Instead, the high frequency fluctuations are dominant in the pressure fluctuations. Therefore, p_4 appears to be at the location where the jet column flaps to the most outward amplitude at t_1 and t_9. From p_5 to p_8, the third kind of pressure behavior is observed, in which the low frequency oscillations—as p_3 exhibits—are modulated with the high frequency fluctuations. This type of pressure variation is due to the occurrence of the flow entrainment from the exterior of the jet stream, induced by the jet flapping motion. However, the pressure variations behave in an out-of-phase manner as compared to those inside the flapping jet.

Flapping Motion as Functions of Impinging Length and Opening Angle

As discussed previously, the flapping motion of the impinging jet occurs when the V-shaped plate is located some distance downstream from the jet exit and the plate has some opening angles. One takes the case of θ = 90 deg as an example while the plate location is variable. Figure 7 depicts the dependence of the flapping jet on the location of the plate. As soon as the jet flaps (see Fig. 7b for $L = 9H$), the pressure transducers on the plate would sense the signals with large amplitudes and specific frequencies, as was observed in the previous section. In this situation, the plate is located within an unstable regime. As for the jet without the flapping, the transducers hardly exhibit any signatures with a preferred low frequency, but there are some kinds of instability waves with high frequency as in Fig. 7a, or random fluctuations in Fig. 7c. The high frequency component in Fig. 7a corresponds to the fundamental shear layer instability frequency as was found in our previous paper[3] at the same conditions in free jet. This is a case in which the plate is located within a stable regime. By collecting all the experimental results for U_j = 10 and 30 m/s, as plotted in Fig. 8, a distinct demarcation boundary for the stable and unstable regimes is constructed for functions of the impinging length and the opening angle of the plate. However, it seems insensitive to the jet exit velocity if comparing the results between 10- and 30-m/s cases. Figure 8 illustrates that as the impinging conditions fall into the unstable regime, a significant periodic flapping motion of the

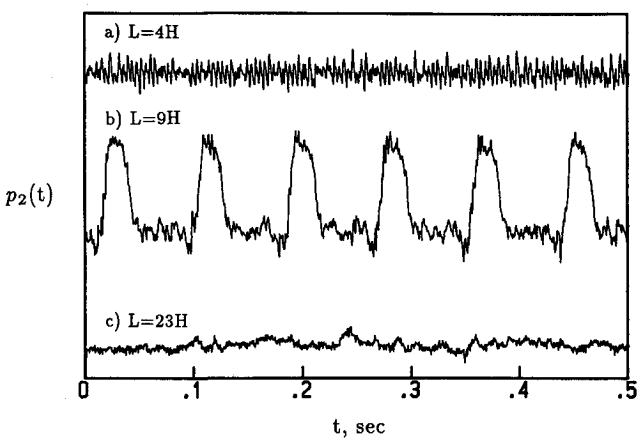

Fig. 7 Examples of dynamic pressure fluctuations at L/H = a) 4, b) 9, and c) 23, for U_j = 10 m/s and θ = 90 deg.

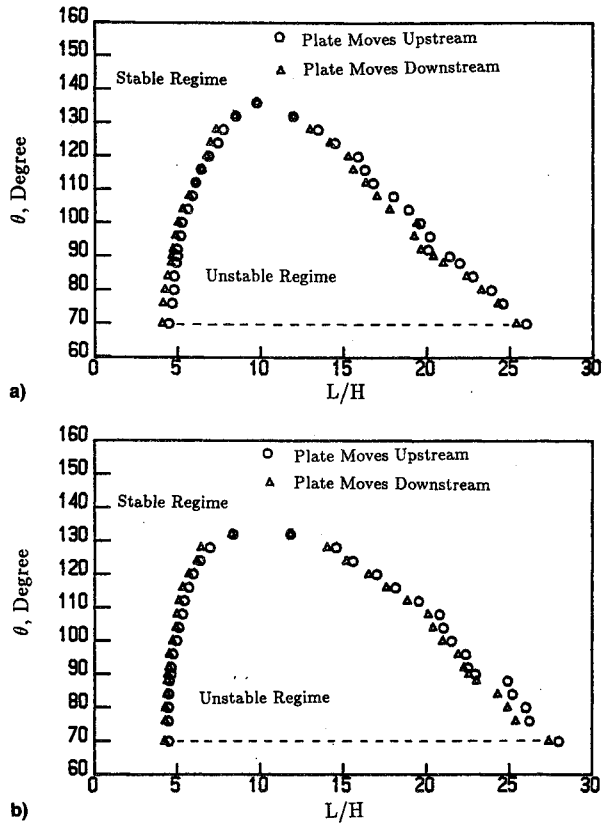

Fig. 8 Demarcation boundary of the stable and unstable regimes for a) U_j = 10 m/s and b) U_j = 30 m/s.

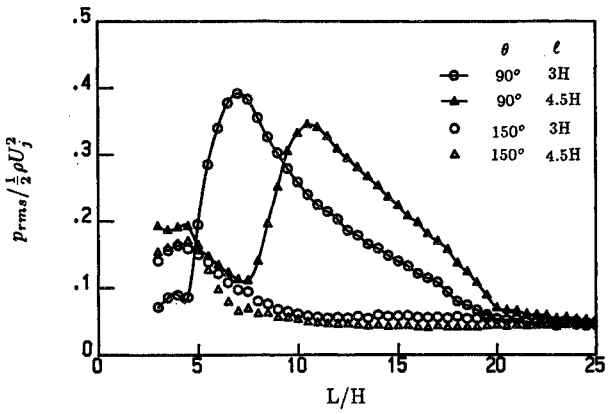

Fig. 9 Root-mean-squared value of pressure fluctuations on the plate in terms of the impinging length for U_j = 10 m/s.

jet column takes place in the flowfield. It also shows that the unstable range decreases with the increase of the opening angle, and disappears as the opening angle is about equal to 138 deg. On the whole, there is an optimal impinging length, about $10H$, for the occurrence of the flapping motion, from which the plate allows a maximum angle variation in the operating jet speed.

To further substantiate the evidence of the demarcation boundary for the jet flapping motion, the amplitudes of the pressure fluctuations on the plate are measured at various plate locations. The results are presented in Fig. 9 for the opening angles fixed at 90 and 150 deg, respectively. It is noted that the sensor locations, $3H$ and $4.5H$, are chosen where the flapping motion is about in the most extreme point. By comparing these two sets of data, it is found that the root-mean-squared (rms) values of the pressure fluctuations significantly increase within the range from $L = 5H$ to $L = 20H$ for the 90-deg case. This range exactly matches the unstable range for the case of θ = 90 deg in Fig. 8a. While the 150-deg case is in the stable regime, no appreciable increase of the amplitude for the pressure fluctuations is found, especially when the plate is located farther downstream. It is noted that, due to the limitation of the traversing mechanism, the V-shaped plate could only vary not less than 70 deg. Further investigations on opening angle plate less than 70 deg are also needed.

Flapping Frequency of Jet Column Motion

The most important characteristics of the flapping motion of the jet column is that there exists a preferred frequency of the flapping jet. This flapping frequency can be determined from the frequency spectra as shown in Fig. 10, which are measured at various points along the plate in the flowfield for U_j = 10 m/s, L/H = 10 and θ = 90 deg. Figure 10a is obtained through a single hot-wire measurement at the jet center, $3H$ downstream from the jet exit. The rest of the spectra are measured by the dynamic pressure transducers located on the plate. It is found that, no matter where the spectra are measured or what kinds of sensor are used, a common preferred frequency exists in these spectra. This common frequency is then defined as the flapping frequency of the jet flapping motion f_F. Notice that both hot-wire and pressure transducers cannot distinguish the jet flapping direction (forward or backward), so that the sensors located at or near the centerline would pick up the flapping jet motion twice in one period of the jet flapping motion. This is the reason why some of the peak frequencies in Figs. 10a and 10b are twice the preferred flapping frequency. Figure 10a also exhibits a local peak frequency near 520 Hz, which corresponds to the fundamental

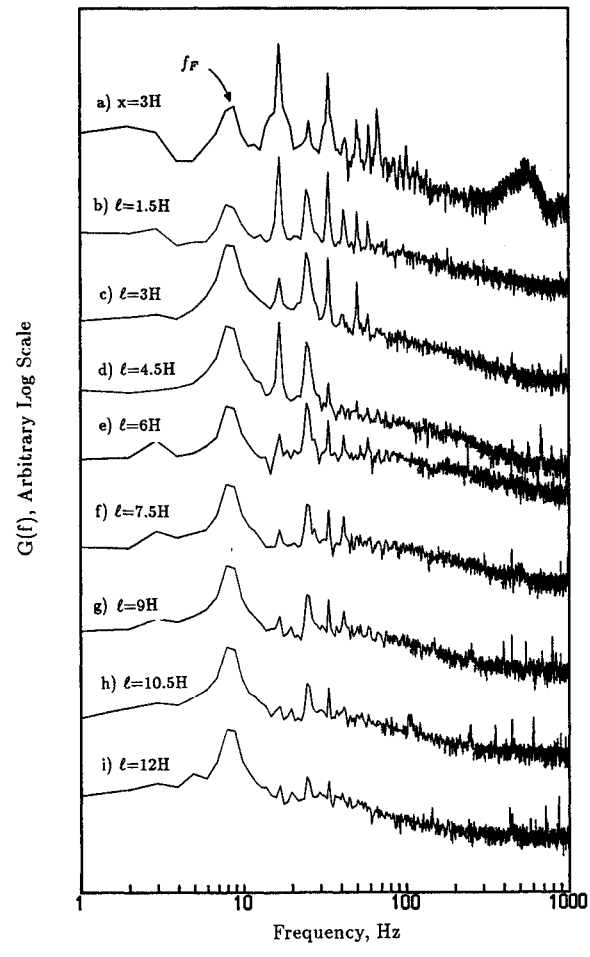

Fig. 10 Frequency spectra measured by a) a hot-wire at the jet center, $3H$ downstream; and by b)–i) dynamic pressure transducers, for U_j = 10 m/s, L/H = 10 and θ = 90 deg.

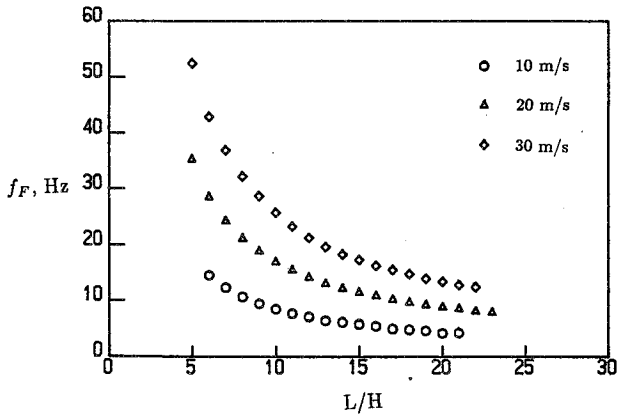

Fig. 11 Flapping frequency in terms of the impinging plate location and the jet exit velocity for θ = 90 deg.

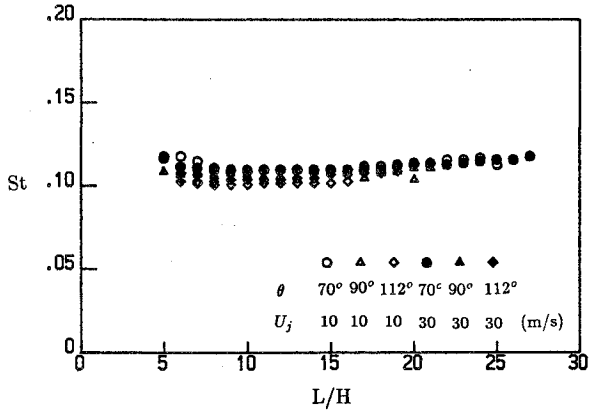

Fig. 12 Flapping Strouhal number in terms of the impinging plate location for various opening angles and jet exit velocities.

frequency of the coherent structures of the shear layers.[3] This frequency is about sixty times the flapping frequency.

The results from the measurements of the pressure variation show that the preferred flapping frequency strongly depends on the location of the plate. The collection of the flapping frequencies with the plate locations is plotted in Fig. 11 for various jet exit velocities and θ = 90 deg. It is found that the flapping frequency is proportional to the jet exit velocity, but is reciprocal of the impinging length. However, if the nondimensional parameter, the so-called Strouhal number $St = f_F L/U_j$ is introduced, the value turns out to be a constant. This is shown in Fig. 12. For the plate closer to the jet exit, the value gets more scattered. In spite of the changes of the jet exit velocity, the opening angle, and the impinging length of the plate, the value slightly varies from 0.1 to 0.12. It shows that the impinging length L is a good characteristic length for scaling. It also demonstrates that a very strong and coherent feedback mechanism exists in the flowfield between the jet exit and the wide-angle plate from the results of the velocity and pressure measurements. Note that a distinct variation of the flow structures takes place from $4H$ to $6H$ of the plate location. This is because the transducer comes across the stable/unstable boundary such that the characteristics of the flow alters its coherent structure properties to the jet flapping motion. This was clearly discussed in the previous sections.

Concluding Remarks

The behavior of flapping motion of an impinging planar jet with a downstream V-shaped plate is studied experimentally by employing velocity and pressure measurements and flow visualization. Despite the presence of the plate in the jet, the large-scaled coherent structures evolved from Kelvin-Helmholtz instabilities are still observed to form regularly as the same fashion in a free jet. However, when the jet column behaves in a periodical motion with time, these coherent structures are then modulated together with the flapping motion of the jet column. This phenomenon is characterized to be in the unstable regime. That is, the jet column appears to flap strongly against both sides of the V-shaped plate. Consequently, the pressure fluctuations on the plate increases several times as the jet flaps. Moreover, a demarcation boundary that distinguishes the stable and the unstable regime are determined as functions of the impinging length and the opening angle of the plate. An optimal impinging length of the plate for maximum opening angle variation exists in the operating Reynolds number range. The flapping frequency is measured to be proportional to the jet exit velocity, and is inversely proportional to the impinging length. When the impinging length is chosen as the length scale, the nondimensional Strouhal number $f_F L/U_j$ is found to remain nearly a constant, 0.11, in the operating jet exit velocity, opening angle, and the impinging distance. As long as the flapping motion takes place, this value is nearly insensitive to the opening angle of the plate.

Acknowledgment

This work is supported by the National Science Council, ROC, under Contract CS77-0210-D006-15.

References

[1]Crow, S. C., and Champagne, F. H., "Orderly Structures in Jet Turbulence," *Journal of Fluid Mechanics*, Vol. 48, Pt. 3, Aug. 1971, pp. 547–591.

[2]Gutmark, E., and Wygnanski, I., "The Planar Turbulent Jet," *Journal of Fluid Mechanics*, Vol. 73, Pt. 3, Feb. 1976, pp. 465–495.

[3]Hsiao, F. B., and Huang, J. M., "On the Evolution of Instabilities in the Near Field of a Plane Jet," *Journal of Fluids A*, Vol. 2, No. 3, 1990, pp. 400–412.

[4]Ho, C. M., and Nosseir, N. S., "Dynamics of an Impinging Jet," *Journal of Fluid Mechanics*, Vol. 105, April 1981, pp. 119–142.

[5]Didden, N., and Ho, C. M., "Unsteady Separation in a Boundary Layer Produced by an Impinging Jet," *Journal of Fluid Mechanics*, Vol. 160, 1985, pp. 235–256.

[6]Hsiao, F. B., Leou, K. M., Huang, J. M., and Chuang, S. H., "The Study of an Impinging Jet About a Flat Plate," *Proceedings of the Fourth Asian Congress of Fluid Mechanics*, edited by N. W. M. Ko and S. C. Kot, Vol. 1, Hong Kong, Aug. 19–23, 1989, pp. A73–76.

[7]Gutmark, E., Wolfshtein, M., and Wygnanski, I., "The Plane Turbulent Impinging Jet," *Journal of Fluid Mechanics*, Vol. 88, Pt. 4, Oct. 1978, pp. 737–756.

[8]Rockwell, D., and Naudascher, E., "Self-Sustained Oscillations of Impinging Free Shear Layers," *Annular Review of Fluid Mechanics*, Vol. 11, 1979, pp. 67–94.

[9]Rockwell, D., "Oscillations of Impinging Shear Layers," *AIAA Journal*, Vol. 21, No. 5, 1983, pp. 645–664.

[10]Staubli, T., and Rockwell, D., "Interaction of an Unstable Planar Jet with an Oscillating Leading Edge," *Journal of Fluid Mechanics*, Vol. 176, March 1987, pp. 135–167.